

## Adsorption and Reaction of Dimethyl Disulfide on the Ni(111) Surface

T. S. Rufael,<sup>†,‡</sup> D. R. Huntley,<sup>\*,§</sup> D. R. Mullins,<sup>§</sup> and J. L. Gland<sup>†</sup>*Department of Chemistry, University of Michigan, Ann Arbor, Michigan 48109, and Oak Ridge National Laboratory, Oak Ridge, Tennessee 37831**Received: September 12, 1997; In Final Form: February 11, 1998*

The adsorption and reactions of dimethyl disulfide,  $\text{CH}_3\text{S}-\text{SCH}_3$ , have been analyzed on the Ni(111) surface using high-resolution electron energy-loss spectroscopy (HREELS), X-ray photoelectron spectroscopy (XPS), low-energy electron diffraction (LEED), Auger electron spectroscopy (AES), temperature programmed desorption (TPD), and deuterium labeling. All of the S–S bonds in dimethyl disulfide (DMDS) are broken below 150 K, forming methyl thiolate ( $\text{CH}_3\text{S}$ ) as the primary surface intermediate. Condensed DMDS desorbs at 166 K. Methane, ethane, and hydrogen are the main desorption products from the reaction of the adsorbed disulfide with Ni(111). The methane desorption following adsorption of DMDS and  $\text{CH}_3\text{SH}$  is remarkably similar. Like methanethiol, total decomposition is favored for DMDS at low coverages, while hydrocarbon formation is the main reaction pathway for higher coverages. The methane desorption profiles for DMDS coadsorbed with hydrogen are similar to those observed from methanethiol coadsorbed with hydrogen. Coadsorption of deuterium with high coverages of DMDS results in an increased temperature (+22 K) for the methane formation reaction, indicating that C–H(D) bond formation is the rate-limiting step in  $\text{CH}_4$  formation at high DMDS coverages. Disproportionation and coupling reactions between the adsorbed thiolates are the main reaction mechanisms for methane and ethane formation, respectively. Analysis of the C 1s XPS peak areas and TPD intensities suggests that by 550 K approximately 85% of the saturated surface thiolate desorbs as gaseous methane and ethane. Annealing a saturation exposure of DMDS (>0.33 ML) on the Ni(111) surface results in a complex LEED pattern as a result of the reconstruction of the top Ni layer. Surface reconstruction starts below room temperature and for S coverages as low as 0.10 ML.

## Introduction

Reactions of simple organosulfur molecules on clean and modified transition metal surfaces have been studied with the goal of understanding the basic surface processes involved in hydrodesulfurization (HDS) catalysis. In particular, experiments on well-characterized single-crystal surfaces elucidated reaction mechanisms and identified surface intermediates that may be important in desulfurization chemistry. The major impact of these types of studies has been to provide data on elementary reaction steps and to identify factors that control reactivity and selectivity. A recent review article outlines in more detail the relationship between fundamental studies on single-crystal surfaces and large-scale processes on supported catalysts.<sup>1</sup> In the present study, the thermal reactions of dimethyl disulfide (DMDS) and derived intermediates have been investigated on the Ni(111) surface using high-resolution electron energy-loss spectroscopy (HREELS), X-ray photoelectron spectroscopy (XPS), low-energy electron diffraction (LEED), and temperature programmed desorption (TPD). Of particular interest in DMDS are the importance of breaking the S–S bonds and the consequences of reducing the amount of available hydrogen compared to methanethiol ( $\text{CH}_3\text{SH}$ ).

Although carbon–sulfur bond activation in methanethiol has been extensively studied on metal surfaces,<sup>1–12</sup> only a few studies involving dimethyl disulfide have been previously reported.<sup>13–18</sup> Fernández et al. have recently reported the

adsorption of DMDS on Ni(111) using near-edge X-ray absorption fine structure (NEXAFS), surface-extended X-ray absorption fine structure (SEXAFS), XPS, photoelectron diffraction, and X-ray standing-wave spectroscopy.<sup>18</sup> They reported that DMDS adsorbs molecularly at 100 K. Methyl thiolate ( $\text{CH}_3\text{S}$ ) is formed following an anneal to 160 K. The methyl thiolate is adsorbed in a mixture of 3-fold sites, and the C–S bond is tilted away from the surface normal toward the surface. The reaction products and yields were not reported in their study. The adsorption of both methanethiol and dimethyl disulfide has been studied on the Au(111) surface<sup>13</sup> using XPS, HREELS, and TPD. Adsorption of methanethiol on the Au(111) surface does not result in S–H bond cleavage, while the S–S bond in the disulfide is reportedly broken at 123 K. No hydrocarbon formation was observed for either adsorbate, and the only desorption products were the original adsorbates. Desorption of chemisorbed molecular methanethiol occurs at near 190 K, while dimethyl disulfide is not observed until 443 K, presumably due to recombination of the thiolate species. A similar study of DMDS and methanethiol has also been performed on Cu(100)<sup>14</sup> using HREELS and TPD. S–H and S–S bond dissociations are observed by 300 K, forming adsorbed methyl thiolate in both cases. A linear Cu–S– $\text{CH}_3$  species is proposed for methanethiol, and a bent Cu–S– $\text{CH}_3$  intermediate is proposed for the disulfide when adsorption takes place at 300 K. In the case of  $\text{CH}_3\text{SH}$  on Cu(100), the primary desorption products are  $\text{H}_2$  (at 335 K),  $\text{CH}_4$  (at 370 K), and  $\text{C}_2\text{H}_6$  (at 420 K). In the case of  $\text{CH}_3\text{S}-\text{SCH}_3$  adsorption, however, both  $\text{CH}_4$  and  $\text{C}_2\text{H}_6$  desorb in a broader peak around 430 K with little or

<sup>†</sup> University of Michigan.<sup>‡</sup> Current address: University of Washington, Seattle WA.<sup>§</sup> Oak Ridge National Laboratory.

no hydrogen evolution. No detailed mechanism was given for the disulfide reactions on Cu(100).

In the present study, the structure and reactivity of DMDS on Ni(111) have been investigated and compared with the chemistry of CH<sub>3</sub>SH on Ni(111) reported earlier.<sup>2</sup> As expected, we find that CH<sub>3</sub>S is the primary surface species present below 200 K for both DMDS and methanethiol. At saturation coverage of either adsorbate, the orientation of the methyl thiolate is similar. The S–C bond is bent toward the surface at low temperature and reorients near the surface normal as the temperature is raised. The main CH<sub>4</sub> desorption peak is similar following adsorption of either DMDS or methanethiol. Methane desorbs at 273 K with a shoulder at 300 K in the case of CH<sub>3</sub>SH, while methane is observed at 268 K with a shoulder at 300 K from DMDS. The main differences between methanethiol and DMDS are that (1) DMDS produces a higher coverage of methyl thiolate, (2) DMDS undergoes a larger fraction of selective as opposed to total decomposition, (3) DMDS exhibits an additional methane formation process at high temperatures, and (4) the rate-limiting step for the methane desorption on a hydrogen-precovered surface is different for the two molecules. The complex chemistry of dimethyl disulfide can be understood using an analogy to earlier studies of CH<sub>3</sub>SH on Ni(111), where high- and low-coordination sites for methyl thiolate were observed.<sup>2</sup> The C–S bond in the thiolate bonded to the high-coordination site is more stable and at a larger angle from the surface than the thiolate in the low-coordination site. Many of the differences observed between methanethiol and dimethyl disulfide chemistry on Ni(111) can be attributed to the higher sulfur coverage, the reduction of free surface H, and the reconstruction of the Ni surface caused by DMDS.

## Experimental Section

This work was performed in three separate systems and on two different Ni(111) crystals. The crystals were about the same dimension, 1 cm in diameter and 1 mm thick. The TPD and deuterium-labeling experiments were performed in the system at the University of Michigan. The HREELS experiments were carried out at ORNL, and the XPS spectra were recorded at the National Synchrotron Light Source (NSLS). Similar TPD results from all three systems confirm that the temperature ranges for reactions and surface selectivities were basically the same so that experimental results can be directly compared.

The temperature programmed desorption experiments were performed in a stainless steel ultrahigh vacuum (UHV) chamber with a working pressure of about  $2 \times 10^{-10}$  Torr. The system was equipped with a multiplexed quadrupole mass spectrometer (QMS) for TPD, a retarding field analyzer for LEED and Auger electron spectroscopy (AES), an ion sputtering gun, and a gas dosing system. The ionizer of the QMS was enclosed in a gold-plated cylinder with a coaxial entrance tube to minimize contribution from the crystal supporting wires. The nickel sample was mounted on two 0.5 mm thick tantalum wires at the tip of an L-shaped manipulator that provided three-coordinate displacements and full rotation. Crystal temperatures of 90–1500 K were attained through liquid nitrogen cooling and resistive heating. The sample temperature was measured using a chromel–alumel thermocouple spot-welded to the back of the crystal.

For the TPD measurements, DMDS dosing was accomplished through a  $\frac{3}{8}$  in. i.d. stainless steel dosing tube with its tip  $\frac{1}{2}$  in. from the sample. The gas flow was controlled by precision variable leak valves. During temperature programmed desorp-

tion the Ni crystal was heated at a rate of 5 K/s. The sample was placed about 1 mm from the mass spectrometer collimator and in direct line of sight to minimize contributions from support wires and background gases. Data were collected with a computer program capable of monitoring 10 masses during a single desorption experiment.

The systems at ORNL and the NSLS were similarly equipped with standard UHV surface-analysis techniques. A high-resolution LK2000 EEL spectrometer was used to record vibrational spectra with typical resolution below 70 cm<sup>-1</sup>. S 2p and C 1s core level photoemission spectra were obtained using a VSW Class 100 hemispherical analyzer stationed on beamline U13UA at the NSLS. A 250 eV excitation was used for S 2p, and 350 eV was used for C 1s. The instrumental resolutions were estimated to be 0.30 and 0.40 eV, respectively.

Dimethyl disulfide (Matheson, 99%) was purified by several freeze–pump–thaw cycles following vacuum distillation. H<sub>2</sub> (Matheson, 99.99%) and D<sub>2</sub> (MSD, 99.5%) were used without further purification. The purity of these gases was checked frequently by mass spectrometry. For the HREELS and soft X-ray photoelectron spectroscopy (SXPS) measurements, DMDS exposure was done by allowing the gas to pass from a large reservoir of DMDS through a 19  $\mu$ m laser-drilled aperture and along a directed dosing tube to the Ni(111) crystal that was positioned immediately in front of the tube. All experiments were performed by adsorbing the gases on the Ni(111) surface near 100 K.

Prior to each experiment, the samples were cleaned by Ar or Ne ion sputtering followed by annealing to 1000 K. The common surface contaminants were sulfur and carbon, which are the decomposition products of DMDS. Surface cleanliness was confirmed by AES, LEED, and occasional blank or hydrogen TPD. At the NSLS, XPS provided a sensitive measure of surface cleanliness.

**Coverage Determination.** Dimethyl disulfide uptake on the Ni(111) surface was monitored using Auger electron spectroscopy, X-ray photoelectron spectroscopy, and low-energy electron diffraction patterns. The sulfur coverages were calibrated by comparing LEED, AES, and XPS results with those obtained in our previous studies of methanethiol and H<sub>2</sub>S on Ni(111).<sup>2,19,20</sup> The only S-containing species that desorbs is multilayer DMDS at 166 K. Therefore, the intensity of the S(152) Auger peak, following TPD or annealing, is proportional to the coverage of chemisorbed DMDS on the Ni surface. Following every TPD, XPS or EELS experiment, the ratio of S(152) to Ni(848) Auger peak-to-peak heights was determined. This ratio increases linearly with increasing DMDS exposure and then plateaus indicating saturation at greater exposures.

Quantitative comparison of the Auger ratios for saturated exposures of CH<sub>3</sub>SH and DMDS on the Ni(111) indicates that the maximum sulfur coverage is 0.33 ML for DMDS, about 30% higher than the saturation coverage from methanethiol.<sup>2</sup> The S 2p XPS peak-area analysis from saturated exposures of CH<sub>3</sub>SH and DMDS yields the identical coverage determination. The LEED patterns following annealing of a saturated Ni(111) surface above 600 K are  $p(2 \times 2)$  or  $(\sqrt{39} \times \sqrt{39})$  for CH<sub>3</sub>SH and  $(5\sqrt{3} \times 2)$  for CH<sub>3</sub>S–SCH<sub>3</sub>. Extensive studies over a wide range of atomic sulfur coverages on Ni(111) found that complex LEED patterns, including the  $(5\sqrt{3} \times 2)$  pattern, are observed in the 0.34–0.40 ML S-coverage range,<sup>19,21</sup> while the  $p(2 \times 2)$  was observed at lower coverages.

To facilitate direct comparisons between the present results for DMDS and the earlier results from methanethiol, the residual chemisorbed sulfur coverages are used to characterize the

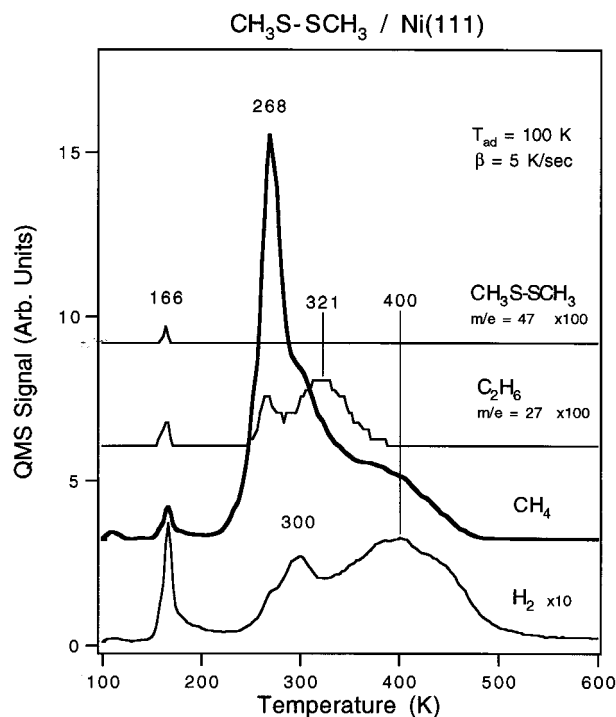


**Figure 1.** Temperature programmed desorption of the products formed from  $\text{CH}_3\text{S}-\text{SCH}_3$  adsorption on a clean Ni(111) surface at 100 K. Data are not corrected for fragmentation. The crystal heating rate was 5 K/s.

DMDS adsorption on Ni(111). For instance, saturation coverage of dimethyl disulfide will be referred to as 0.33 ML of DMDS instead of 0.165 ML of DMDS. The S-S bond in dimethyl disulfide breaks below 150 K prior to any desorption, resulting in adsorbed  $\text{CH}_3\text{S}$ , which behaves very much like the methyl thiolate from  $\text{CH}_3\text{SH}$  on Ni(111). Therefore, the DMDS coverages indicated represent the thiolate or chemisorbed sulfur coverage resulting from DMDS adsorption on the Ni(111) surface.

## Results

**Reaction Products.** The thermal desorption products following a high exposure of dimethyl disulfide on a Ni(111) surface are dimethyl disulfide, methane, hydrogen, and a small amount of ethane as shown in Figure 1. At high coverages of DMDS on Ni(111), methane desorbs at 268 K, with a broad high-temperature tail, and hydrogen desorbs in two broad peaks at 300 and 400 K. A very small amount of ethane is observed at 320 K. The DMDS peak at 166 K is due to multilayer desorption. Multilayer desorption temperatures of 166 K are also observed for DMDS on Pt(111) and Ni(100).<sup>22</sup> Sexton and Nyberg<sup>14</sup> reported 140 K as the multilayer desorption temperature for DMDS on the Cu(100) surface, though they observed an unexplained bigger and sharper peak at 170 K.

The bottom panel in Figure 2 illustrates TPD profiles of  $\text{H}_2$  as a function of DMDS exposure. For low DMDS coverages, hydrogen desorbs from the Ni(111) surface in a single symmetric peak about 390 K. This peak matches the desorption-limited peak observed when  $\text{H}_2$  is adsorbed on the clean Ni(111) surface.<sup>23</sup> As the DMDS exposure is increased, the intensity of this desorption-limited hydrogen peak goes through a maximum and shifts toward lower temperatures, reaching a minimum desorption temperature of around 300 K. In the  $\text{CH}_3\text{SH}/\text{Ni}(111)$  case, the desorption-limited  $\text{H}_2$  peak is observed at 335 K.<sup>2,12</sup> With increasing DMDS coverage, a sharp reaction-

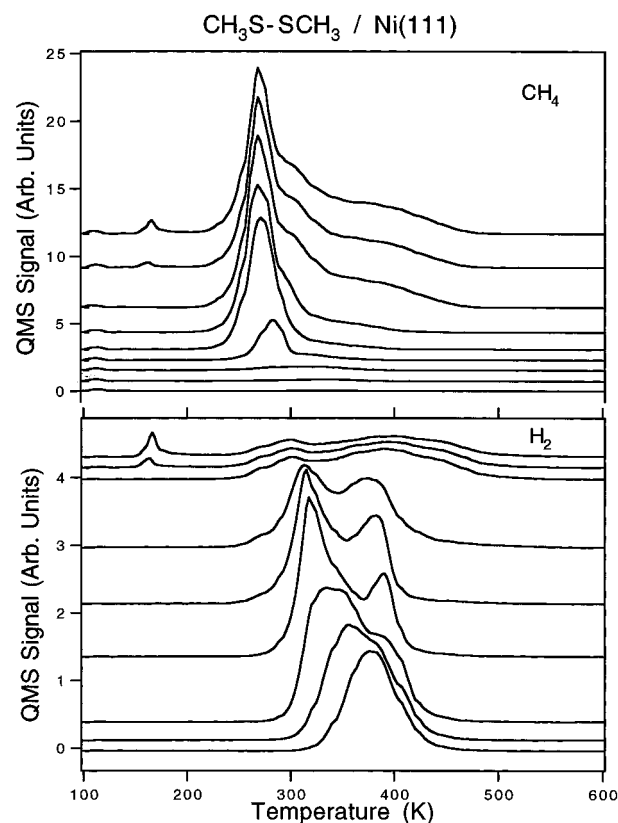


**Figure 2.** Temperature programmed desorption profiles of  $\text{H}_2$  (bottom) and  $\text{CH}_4$  (top) from Ni(111) as a function of DMDS exposure. In each panel, the coverages (in ML) correspond to 0.07, 0.10, 0.13, 0.165, 0.23, 0.28, 0.33, 0.50, and 0.82, drawn from bottom to top.

limited  $\text{H}_2$  peak becomes visible around 400 K. This  $\text{H}_2$  desorption peak shows a maximum intensity at a DMDS coverage of about 0.17 ML before becoming a broad peak with a desorption temperature of 350–500 K as saturation is approached.

The TPD profiles of  $\text{CH}_4$  as a function of DMDS coverage are shown in the top panel of Figure 2. Methane first appears when the DMDS coverage is about 0.15 ML and desorbs in a single peak at about 290 K. With increasing coverage, this feature shifts to lower temperatures and grows into a strong peak with a maximum at 268 K. This methane desorption peak is very similar to the peak observed from  $\text{CH}_3\text{SH}$  on Ni(111) at 273 K.<sup>2</sup> Above 0.20 ML of DMDS, a high-temperature shoulder emerges at around 300 K, as previously observed in the  $\text{CH}_3\text{SH}/\text{Ni}(111)$  case. However, an additional broad methane desorption feature between 350 and 470 K is observed for the highest coverages of DMDS, accompanied by a reaction-limited high-temperature hydrogen desorption peak.

At high DMDS coverages, a small amount of  $\text{C}_2\text{H}_6$  ( $\leq 1\%$  of methane peak) desorbs in a peak with a maximum at 266 K. This peak is similar to the 270 K ethane peak formed from  $\text{CH}_3\text{SH}/\text{Ni}(111)$ . In addition, a more intense and broader ethane desorption feature, not seen in  $\text{CH}_3\text{SH}/\text{Ni}(111)$  TPD, is observed at 321 K.

Figure 3 shows the relative desorption yield curves for  $\text{H}_2$  and  $\text{CH}_4$  as a function of DMDS coverage. At less than 0.15 ML coverage, decomposition of the adsorbates to atomic species is the sole reaction pathway as indicated by the absence of  $\text{CH}_4$  in the desorption products and the initial increase in the hydrogen desorption yield with increasing exposure. Above 0.15 ML, the amount of  $\text{CH}_4$  increases rapidly as the DMDS coverage increases, and the calibrated desorption yields indicate

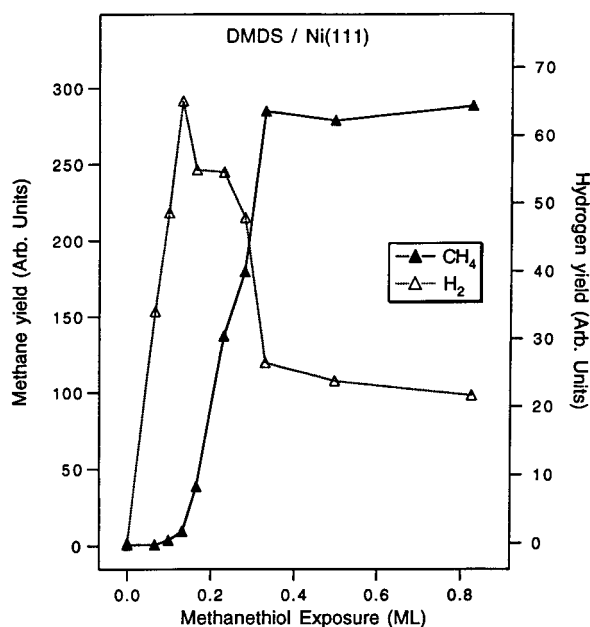


**Figure 3.** Hydrogen and methane desorption yield curves as a function of initial DMDS exposure to Ni(111) surface.

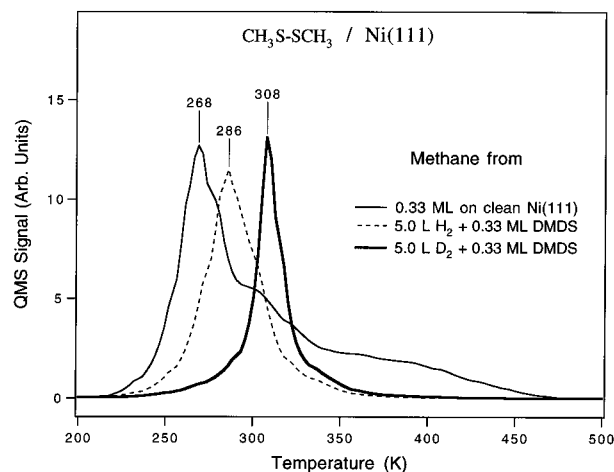


**Figure 4.** Effects of preadsorbed hydrogen (dashed line) and deuterium (bold line) on the methane desorption profiles for 0.33 ML of DMDS. In the case of the deuterium-predosed surface, the plotted methane desorption profile is the sum of all isotopic combinations ( $d_0$ – $d_4$ ). The heating rate was 5 K/s.

that  $\text{CH}_4$  becomes the dominant reaction product at coverages greater than 0.25 ML. The amount of  $\text{H}_2$  that desorbs decreases as the  $\text{CH}_4$  increases.

When  $\text{H}_2$  is preadsorbed on Ni(111), the low-temperature methane peak temperature for DMDS increases 18 K from 268 K to 286 K as shown in Figure 4. This peak appears at the same temperature as methane desorption from  $\text{CH}_3\text{SH}$  on an  $\text{H}_2$ -predosed Ni(111) surface. In both cases, methane formation is shifted to higher temperatures by coadsorbed hydrogen. The high-temperature tail of methane in the case of DMDS also disappears on the  $\text{H}_2$ -predosed surface. The ethane peak temperature increases by 20 K to 286 K (data not shown). The second desorption feature of ethane (at 321 K) disappears in the presence of surface hydrogen.

When deuterium is preadsorbed on the Ni(111) surface prior to DMDS adsorption, two major changes are observed compared to the  $\text{H}_2$  preadsorbed case. First, as seen in Figure 4, the methane desorption temperature is 22 K higher (308 K) in the presence of deuterium instead of hydrogen, a clear indication

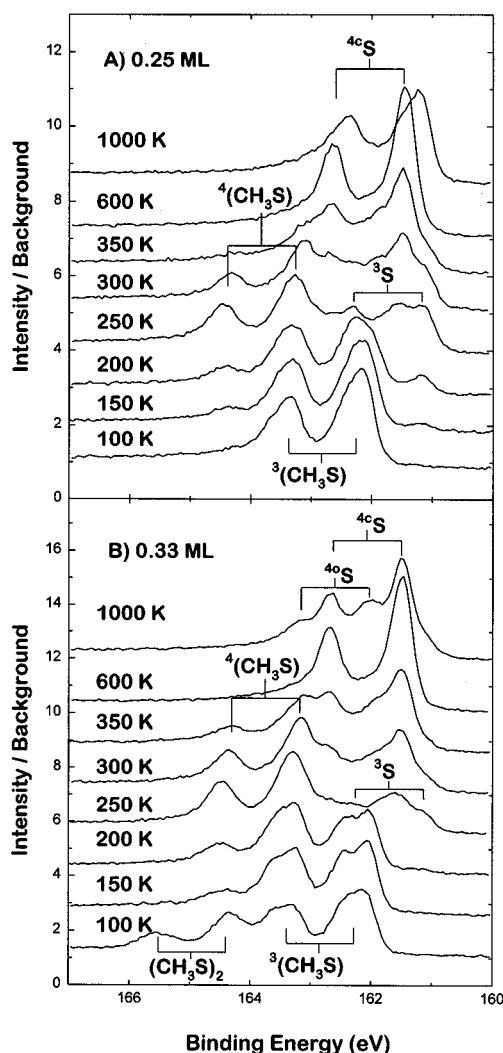


**Figure 5.** S 2p photoelectron spectra for (A) 0.25 ML and (B) 0.33 ML of DMDS adsorbed on the Ni(111) at 100 K. The samples were annealed at the indicated temperatures for 60 s, then quenched before data were collected. The superscripts on the peak labels indicate the coordination of the adsorption site.

of an isotope effect. Second, the fwhm of this methane peak in the presence of  $\text{D}_2$  is smaller than in the presence of  $\text{H}_2$ . Multiple deuterium incorporation is observed, since desorption is detected at all masses from  $m/e = 15$ – $20$  with the largest signal being at  $m/e = 17$  ( $\text{CH}_3\text{D}$ ). However, incorporation of more than one D atom implies either significant H/D exchange in the methyl hydrogens during/prior to the hydrogenolysis of C–S bond, or the existence of partially dehydrogenated surface species. Exposing the surface to  $\text{H}_2$  or  $\text{D}_2$  after DMDS adsorption does not affect the methane and hydrogen desorption features. This indicates that DMDS blocks the adsorption of  $\text{H}_2$  or  $\text{D}_2$ .

**X-ray Photoelectron Spectroscopy.** S 2p and C 1s core level photoemission spectra are shown in Figures 5 and 6, respectively. When describing the S 2p spectra, only the peak position of the S  $2p_{3/2}$  component of the spin–orbit doublet will be given for simplicity. The peak positions and assignments for the S 2p and C 1s spectra are summarized in Table 1. In all cases the spectra were obtained by heating for 60 s at the indicated temperature and quenching the sample to about 100 K for measurement.

S 2p spectra from 0.25 ML of DMDS on Ni(111) are shown in Figure 5A. The peaks that occur in the spectra are the same

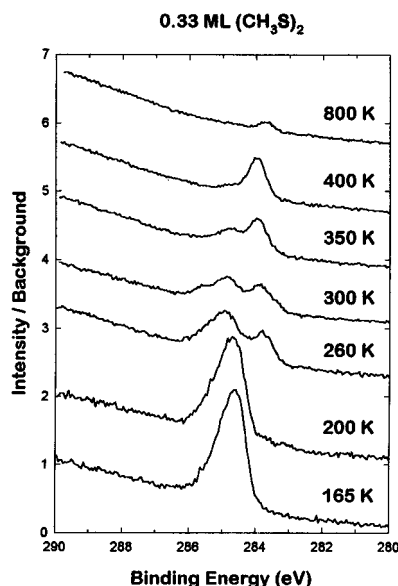


**Figure 6.** C 1s photoelectron spectra for a multilayer coverage of DMDS adsorbed on the Ni(111) at 100 K. The sample was annealed at the indicated temperatures for 60 s, then quenched before data were collected.

regardless of whether the sample is exposed to 0.25 ML of  $\text{CH}_3\text{SH}$  or DMDS.<sup>2</sup> At 100 K a single S 2p doublet occurs with a S 2p<sub>3/2</sub> binding energy of 162.30 eV. This signal is assigned to a  $\text{CH}_3\text{S}$  intermediate. The peaks are asymmetric, indicating that there is probably a second state at a slightly higher binding energy. At 150 and 200 K, two new S 2p states appear with S 2p<sub>3/2</sub> peak positions at 161.15 and 163.30 eV. The low binding energy state is attributed to atomic S in a 3-fold site,<sup>10,20</sup> while the higher binding energy state is assigned to  $\text{CH}_3\text{S}$  in a higher-coordination site than is observed at low temperatures.<sup>2,10</sup> The intensity of the original thiolate peak near 162.30 eV has decreased significantly by 250 K, while the high-coordination thiolate state at 163.30 eV and a second atomic S state at 161.55 eV, assigned to atomic S in a reconstructed 4-fold site,<sup>10,20</sup> both increase in intensity. At 300 K, the thiolate state at 163.30 eV decreases in intensity while the peak due to atomic sulfur in the reconstructed site becomes the most prominent in the spectrum. At 350 K, all of the peaks assigned to thiulates have disappeared while the peaks attributed to chemisorbed S in the 4-fold sites continue to increase. By 600 K, all of the sulfur appears to be in the reconstructed 4-fold sites. Annealing to 1000 K causes the atomic S peak at 161.15 eV to reappear and the peak at 161.55 eV to diminish.

The spectra from 0.33 ML of DMDS (Figure 5B) contain additional features compared with spectra at the lower coverage. At 100 K, a new state appears at 164.35 eV and is attributed to intact DMDS. This state disappears when the sample is annealed to 150 K. Since the integrated intensity of all of the S 2p peaks is the same at 100 and 150 K, it is evident that some DMDS adsorbs molecularly in the first monolayer and the S–S bond dissociates below 150 K. Two peaks are observed at 162.10 and 162.50 eV, and both are attributed to  $\text{CH}_3\text{S}$  species. Above 150 K, the  $\text{CH}_3\text{S}$  peak at 163.30 eV appears and is again attributed to a thiolate in a higher-coordination site. The atomic S peak at 161.15 eV does not appear until the sample is annealed to 250 K, in contrast to the data for 0.25 ML of DMDS where atomic S is evident at 150 K. The spectra at 250 K are similar in Figure 5, except that at the higher coverage, the populations of both atomic S and thiulates in the reconstructed high-coordination sites are larger

than at lower coverage. At 350 K for 0.33 ML of DMDS, the state due to thiulates in the high-coordination sites at 163.30 eV is still evident. The atomic sulfur states below 162 eV evolve as they did for lower coverage. The peak at 161.55 eV becomes more prominent as the temperature is increased. At 1000 K an additional atomic S peak at 162.10 eV appears.

As seen in Figure 5, the thiolate peaks in the S 2p spectra of DMDS below 200 K are split. The degree of splitting is related to coverage. The spectra of methyl thiolate from either 0.25 ML of DMDS or  $\text{CH}_3\text{SH}$  show a distinct broadening and asymmetry compared with spectra at lower coverages. The increase in coverage above 0.25 ML causes the broadened peak to actually split into two resolvable peaks. One possible explanation is that the reconstruction (*vide infra*) of the Ni surface observed for DMDS begins at low temperatures, resulting in multiple adsorption sites on a structurally inhomogeneous surface.

C 1s spectra from a multilayer of DMDS annealed to various temperatures are shown in Figure 6. A single peak from  $\text{CH}_3\text{S}$  occurs at 284.5 eV and is evident from 165 to 350 K. Atomic C at 283.7 eV first appears at near 220 K (data not shown). The small shoulder at 285.5 eV that is clearly visible in the 300 K spectrum is assigned to <0.02 ML of CO that adsorbed from the ambient during sample preparation. The atomic C coverage at 400 K is estimated to be  $0.09 \pm 0.02$  ML on the basis of the C 1s intensities from saturation coverages of DMDS and  $\text{CH}_3\text{SH}$  that are assumed to be 0.33 and 0.25 ML, respectively. The C 1s intensity decreases to 0.05 ML at 600 K and 0.02 ML at 800 K.

**High-Resolution Electron Energy-Loss Spectroscopy.** The identity and structure of the adsorbed species that form following DMDS adsorption on the Ni(111) surface were also investigated as a function of temperature and coverage using high-resolution electron energy-loss spectroscopy. The spectra of the intermediates formed by thermal decomposition of the adsorbed DMDS were obtained by heating to the indicated temperatures and quenching the sample to 100 K for measurement. Temperatures were selected on the basis of the TPD and XPS results.

The vibrational modes of physisorbed DMDS are summarized in Table 2 and exhibit good agreement with the liquid-phase IR frequencies of DMDS<sup>24</sup> and with spectra from condensed DMDS on other surfaces.<sup>13,14</sup> The S–S–C bending and the S–S stretch modes are observed at 235 and 495  $\text{cm}^{-1}$ , in good agreement with the liquid IR values of 241 and 511  $\text{cm}^{-1}$ , respectively. The C–S stretch frequency occurs at 695  $\text{cm}^{-1}$ , in excellent agreement with the liquid-phase value of 691  $\text{cm}^{-1}$ . The methyl rocking mode is present at 960  $\text{cm}^{-1}$ , while the losses at 1315 and 1430  $\text{cm}^{-1}$  are assigned to the methyl deformation modes. The C–H stretching modes appear at 2915 and 2990  $\text{cm}^{-1}$ .

The HREELS spectra of a saturated overlayer of DMDS are summarized in Table 2 and shown in Figure 7 as a function of annealing temperature. The sulfur coverage following the annealing set was approximately 0.34 ML. At 90 K, the spectra exhibit peaks assigned to the C–S stretching mode at 695  $\text{cm}^{-1}$ , the methyl rocking mode at 960  $\text{cm}^{-1}$ , the symmetric and asymmetric methyl deformations at 1315 and 1430  $\text{cm}^{-1}$ , and the C–H stretching modes at 2915–2990  $\text{cm}^{-1}$ . The losses associated with the S–S bond, the  $\nu(\text{S–S})$  and the  $\delta(\text{S–S–C})$  modes of molecular DMDS, are absent for the chemisorbed layer, while the remaining vibrational modes are still present. This vibrational spectrum shows all the characteristic frequencies of adsorbed  $\text{CH}_3\text{S}$ .<sup>2,7–9,13,14</sup>

**TABLE 1: S 2p and C 1s Binding Energies for CH<sub>3</sub>SH and DMDS on Ni(111)**

	species	binding energy (eV)	assignt
S 2p <sub>3/2</sub>	atomic S on Ni(111)	161.15 ± 0.05	fcc 3-fold hollow site
	atomic S on Ni(111)	161.55	"closed" 4-fold hollow site <sup>a</sup>
	atomic S on Ni(111)	162.10	"open" 4-fold hollow site <sup>a</sup>
	atomic S on Ni(001)	161.55	4-fold hollow site
	CH <sub>3</sub> S from DMDS on Ni(111)	162.1–162.5	fcc 3-fold hollow site
	CH <sub>3</sub> S from DMDS on Ni(111)	163.30	"closed" 4-fold hollow site
	CH <sub>3</sub> S from CH <sub>3</sub> SH on Ni(111)	162.30	fcc 3-fold hollow site
	CH <sub>3</sub> S from CH <sub>3</sub> SH on Ni(111)	163.30	"closed" 4-fold hollow site
	CH <sub>3</sub> S from CH <sub>3</sub> SH on Ni(001)	163.35	4-fold hollow site
	CH <sub>3</sub> S on Ni(111)	284.5 ± 0.1	
C 1s	atomic C on Ni(111)	283.7	

<sup>a</sup> Reference 20.**TABLE 2: Vibrational Mode Assignments for Multilayer Dimethyl Disulfide on Ni(111)<sup>a</sup>**

assignt	liquid DMDS <sup>b</sup>	100 K	150 K	250 K	CH <sub>3</sub> S/Ni(111) <sup>c</sup>	ML DMDS/Cu(100) <sup>d</sup>
δ(S–S–C)	241 276	235				300
ν(Ni–SCH <sub>3</sub> )		400	310	295	325	
ν(Ni–S)				355		
ν(S–S)	511	495				
ν(C–S)	691	695	660	660	642, 690	680
ρ(CH <sub>3</sub> )	955	960	930	930	922	960
δ <sub>s</sub> (CH <sub>3</sub> )	1303	1315	1290	1290	1269	1320
δ <sub>a</sub> (CH <sub>3</sub> )	1415	1430	1445	1445	1410	1450
	1430					
ν <sub>s</sub> (C–H)	2915	2915	2900	2915	2915	2930
ν <sub>a</sub> (C–H)	2986	2990	2990	2970	2974	3020

<sup>a</sup> All frequencies in cm<sup>-1</sup>. <sup>b</sup> IR spectra for liquid dimethyl disulfide (ref 24). <sup>c</sup> Monolayer-adsorbed CH<sub>3</sub>S/Ni(111) at 140 K (ref 2). <sup>d</sup> Monolayer DMDS on Cu(100) at 300 K (ref 14).

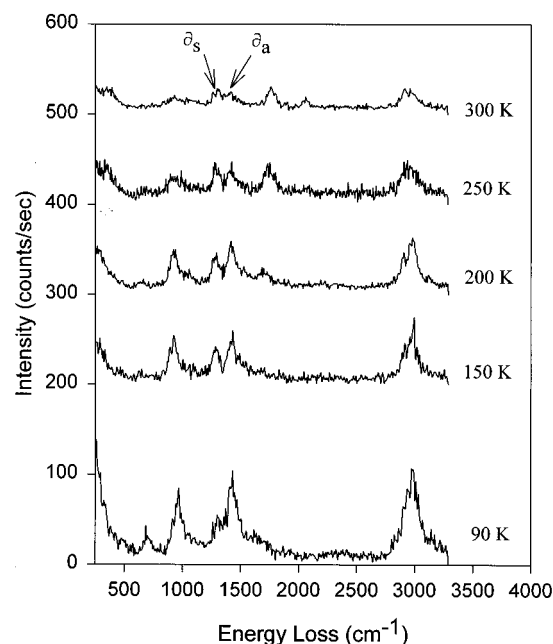


**Figure 7.** High-resolution electron energy-loss spectra for saturation coverage of DMDS on Ni(111) adsorbed at 90 K. The sample was annealed at the indicated temperature for 60 s and quenched to 100 K for data collection. All data were collected for specular scattering, and the spectral resolution was approximately 50–60 cm<sup>-1</sup>.

Annealing the surface above 150 K results in a decrease in the ratio of the symmetric to the asymmetric methyl deformation and C–H stretching modes but no other significant changes in the spectrum. This indicates reorientation of the methyl groups relative to the surface normal. A simple application of the dipole selection rule suggests that the S–C bond above 150 K is more tilted toward the surface normal than at 100 K. A similar

decrease in the ratio of the symmetric to the asymmetric methyl deformation and C–H stretching modes is also observed for CH<sub>3</sub>S from methanethiol on Ni(111).<sup>2,10</sup>

Heating the surface above 200 K causes loss of some of the surface species due to the desorption of methane from the surface. As a result, the intensities of the modes associated with carbon are substantially attenuated. C–S bond activation has occurred as indicated by the appearance the Ni–S stretching mode (355 cm<sup>-1</sup>). This loss could potentially be assigned to a Ni–CH<sub>x</sub> stretch mode, since a ν(Ni–CH<sub>3</sub>) mode was reported at 370 cm<sup>-1</sup> on the Ni(111) surface.<sup>25</sup> However a more likely assignment is the Ni–S stretch, since the TPD and XPS data indicate that about 70% of the C has desorbed by this temperature while a large coverage of atomic S has formed.

Further heating of the saturated DMDS above 500 K results in more desorption of methane, ethane, and hydrogen, leaving a complex (5√3 × 2) S structure on the Ni surface. This sulfur structure on Ni(111) has been determined to be due to the reconstruction of the top Ni layer forming a distorted Ni(100) c(2 × 2) S structure.<sup>10,17,19,20,26</sup> Figure 8 shows the vibrational spectra for 0.33 and 0.15 ML of DMDS on Ni(111) surface after annealing to 550 K. The vibrational spectrum from the 0.33 ML DMDS-covered surface at 550 K or higher shows only one intense mode at 315 cm<sup>-1</sup>, which corresponds to the Ni–S stretch from adsorbed atomic sulfur. The LEED patterns observed from the 0.15 ML DMDS-covered surface were not well defined. However, weak spots appear that look like those from the early stages of the (5√3 × 2) S or c(5√3 × 9) C structure, suggesting that surface reconstruction may well be underway even at a DMDS coverage of 0.15 ML. The vibrational spectrum of this surface indicates the absence of any molecular fragments, since the only mode observed is the ν(Ni–S) mode at 375 cm<sup>-1</sup>. For comparison, the spectrum for a saturation coverage of methanethiol on Ni(111) at 800 K,

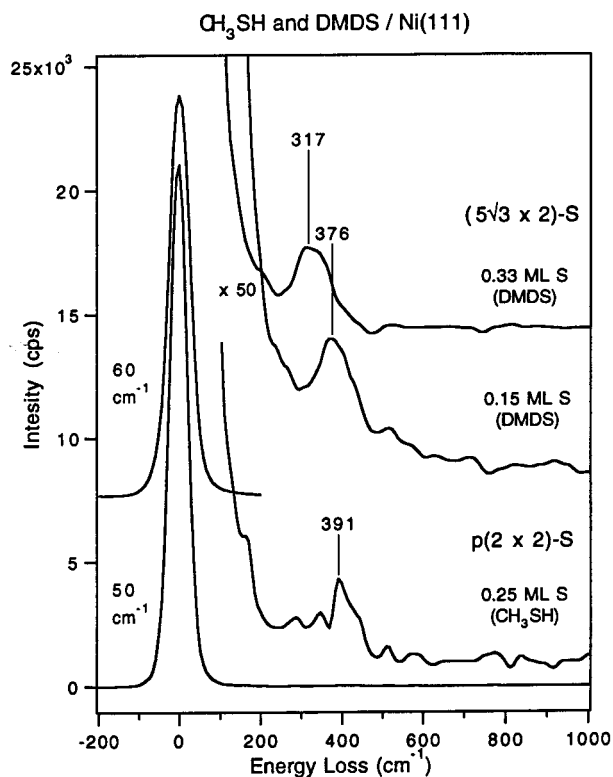


**Figure 8.** Ni–S stretching frequencies for atomic sulfur having  $p(2 \times 2)$  S structure on Ni(111) as a result of (a) saturated  $\text{CH}_3\text{SH}$  annealed to 800 K, (b) 0.15 ML of DMDS annealed to 550 K, and (c) the corresponding Ni–S stretching mode for atomic sulfur having the  $(5\sqrt{3} \times 2)$  S structure as a result of saturation coverages of DMDS on the Ni(111) surface.

which formed a sharp  $p(2 \times 2)$  S structure with 0.25 ML, is included in the figure and shows a peak at  $390\text{ cm}^{-1}$ . The  $\nu(\text{Ni}-\text{S})$  frequencies for pure S from  $\text{H}_2\text{S}$  annealed on Ni(111) are  $410\text{ cm}^{-1}$  at low S coverage and  $325\text{ cm}^{-1}$  at high S coverage.<sup>20</sup> Ni–S stretching frequencies of about 350 and 365  $\text{cm}^{-1}$  have been reported previously for  $c(2 \times 2)$  and  $p(2 \times 2)$  S structures on the Ni(100) surface.<sup>27</sup>

## Discussion

**Identity and Structure of Adsorbed Species.** Dimethyl disulfide forms the same intermediates on Ni(111) as methanethiol. For S coverages of  $\leq 0.25$  ML, all of the DMDS decomposes to form methyl thiolate at 100 K. The vibrational spectra clearly indicate the presence of methyl thiolate, since they exhibit the same features as methyl thiolate adsorbed on various metal surfaces following methanethiol exposure.<sup>2,3,7–9,14</sup> A single state of methyl thiolate is formed at low temperatures, as is evident from the S 2p spectrum (Figure 5A), which shows only a single state of S at 100 K with the same binding energy as that of  $\text{CH}_3\text{S}$  from  $\text{CH}_3\text{SH}$  (see Table 1).

Detailed examination of the TPD spectra from DMDS supports the conclusion that methyl thiolate is the primary surface intermediate. First, we observe  $\text{C}_2\text{H}_6$  and not  $\text{C}_2\text{H}_4$  or  $\text{C}_2\text{H}_2$ , suggesting that the methyl group stays intact and that the thioformaldehyde species reported on Pt(111) is not formed on Ni(111). The coincidence of the methane desorption temperatures with the observed changes in the XPS and HREELS spectra provides further evidence that the thiolate is the primary reaction intermediate for methane formation. The isotopic distributions of the methane formed from DMDS on deuterium-preadsorbed Ni(111) show that nearly 75% of the

methane desorbs as  $\text{CH}_3\text{D}$ . This also suggests that most of the methyl groups remain intact during the hydrogenolysis.

The appearance of two distinct S 2p states with binding energies above 162 eV in the temperature range 150–350 K provides clear evidence for multiple thiolate adsorption sites. Two adsorption sites for methyl thiolate were observed in the methanethiol study on the Ni(111) surface<sup>2</sup> where a lower-coordination site is populated upon adsorption at 100 K and a higher-coordination site becomes populated after annealing to  $>200$  K. These two adsorption states were initially assigned to thiolates in bridge and hollow sites, respectively. Recent X-ray standing-wave and photoelectron diffraction experiments indicate that the lower-coordination species (S  $2p_{3/2}$  binding energy of 162.30 eV) observed at low temperature is methyl thiolate adsorbed in a 3-fold site.<sup>10,18</sup> The photoelectron diffraction experiments also indicate that the species with the S  $2p_{3/2}$  binding energy of 163.30 eV observed above 200 K is not adsorbed in a 3-fold site.<sup>10</sup> The similarity of the S 2p binding energies for  $\text{CH}_3\text{S}$  on Ni(111) and  $\text{CH}_3\text{S}$  on Ni(100) (see Table 1) suggests that the highest binding energy thiolate on Ni(111) is in a reconstructed 4-fold site, since the thiolate on Ni(001) has been shown to be adsorbed in the 4-fold site.<sup>28</sup> We therefore propose that the thiolates observed at low temperatures and binding energy (162.1–162.5 eV) from DMDS are adsorbed in 3-fold hollow sites and that the thiolates at higher temperature and binding energy (163.3 eV) are adsorbed in reconstructed 4-fold sites (see Table 1), exactly analogous to what was observed from methanethiol adsorption on the same surface.

The relative intensities of the symmetric and asymmetric methyl deformation and C–H stretching modes indicate that the thiolate species are tilted at low temperature and reorient at higher temperatures. For adsorbed methyl thiolate with a C–S bond along the surface normal, the symmetric modes are dipole-allowed while the asymmetric modes are dipole-forbidden. The opposite would be true for a  $\text{CH}_3\text{S}$  with its C–S bond parallel to the surface. However, for a tilted geometry both modes may be active. For the methyl thiolate at 175 K (Figure 7) both the asymmetric deformation mode at  $1415\text{ cm}^{-1}$  and the C–H stretching mode at  $2990\text{ cm}^{-1}$  are very intense, indicating that the C–S bond is highly tilted toward the surface at this temperature. Above 200 K, the relative intensity of the symmetric modes at  $1315$  and  $2915\text{ cm}^{-1}$  increases, suggesting that the C–S bond reorients along the surface normal. This reorientation is similar to what has been reported previously for methanethiol on Ni(111)<sup>2</sup> and is consistent with the XPS data, which show a change in adsorption site over the same temperature range. Further support for this hypothesis comes from recent photoelectron diffraction experiments on methyl thiolate<sup>10</sup> from methanethiol, which demonstrate that the C–S bond is tilted with respect to the surface normal for the thiolate adsorbed in the 3-fold site and is oriented along the surface normal for the thiolate in the reconstructed site.

**Reaction of the Methyl Thiolate Intermediate.** The reactions of  $\text{CH}_3\text{S}-\text{SCH}_3$  are more complex than the reactions of  $\text{CH}_3\text{SH}$  on the Ni(111) surface. There are three distinct methane formation processes evident in the methane TPD curve in Figure 1. These three processes are manifested in (1) the intense methane peak at 268 K, (2) the overlapping peak around 300 K, and (c) the broad feature in the 300–450 K region. The low-temperature methane formation process is similar to the hydrogenolysis of methyl thiolate (3-fold site) observed for methanethiol on Ni(111). Methane desorption at intermediate temperature, also observed from  $\text{CH}_3\text{SH}$ , comes from the

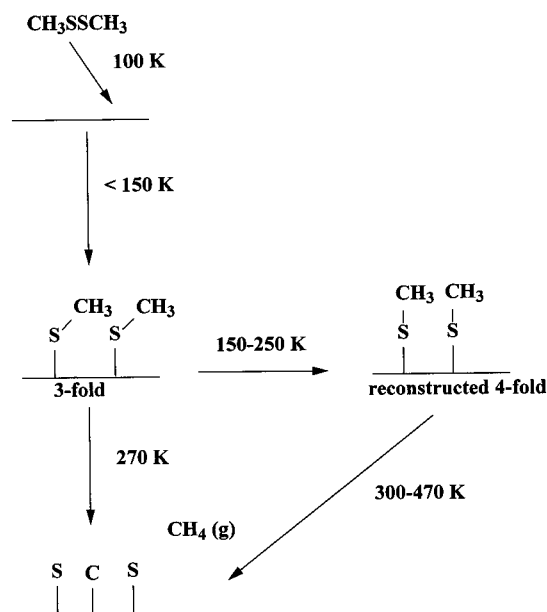


**Figure 9.** Proposed reaction mechanism for a high-coverage dimethyl disulfide with a Ni(111) surface.

reaction of methyl thiolate adsorbed on the reconstructed 4-fold site. High-temperature methane production, not seen in methanethiol adsorption, arises from thiolates that are apparently stabilized by the higher S coverages obtained from DMDS. A summary of the proposed reaction mechanisms for DMDS on the clean Ni(111) surface is shown in Figure 9.

The fact that the methane desorption peaks are almost identical in both the thiol and the disulfide for the main methane peak at 268 K indicates that C–H bond scission does not limit the methane formation rates at that temperature. This methane desorption peak is attributed to hydrogenolysis of the methyl thiolate adsorbed in the 3-fold site by surface hydrogen, analogous to the methanethiol/Ni(111) system,<sup>2</sup> where methane desorption is formed at nearly the same temperature. The S 2p spectra indicate that the methyl thiolate adsorbed in the 3-fold sites is essentially gone by 300 K. Therefore, the methane desorption above 300 K must come from the methyl thiolates adsorbed on the reconstructed sites. The shift in desorption temperature from 268 and 300 K for the two types of thiolates may be related both to changes in surface structure and to adsorbate–adsorbate interactions.

The primary effect of preadsorbing hydrogen on the Ni(111) surface prior to DMDS exposure is a shift in the 268 K methane desorption feature by 18 K to higher temperature. Two possible explanations for this shift are that the preadsorbed H blocks active sites and therefore stabilizes the thiolate to higher temperature and that the chemisorbed H assists in the surface reconstruction, causing the thiolate to shift into the more stable 4-fold sites. Some stabilization of methyl thiolate by hydrogen is evident in the XPS data, where C–S bond scission is observed at lower temperature for DMDS than for methanethiol at the same S coverage. Apparently, the sulfhydryl hydrogen acts to block C–S bond scission in the methanethiol case.

Although both surface deuterium and hydrogen cause the methane desorption feature to shift toward higher temperature, a much larger shift (to 308 K, for all isotopic combinations) is observed for deuterium in the case of DMDS adsorption. Interestingly, in the methanethiol case, the methane desorption peak did not show an isotope shift when preadsorbed deuterium was substituted for hydrogen.<sup>2</sup> It is not clear why there is an isotope effect for DMDS and not CH<sub>3</sub>SH. This difference may

be related to coverage, since at saturation, the thiolate coverage is significantly greater for DMDS. The observed isotope effect may also be related to subtle differences in the surface structure during the decomposition of CH<sub>3</sub>SH and DMDS. It can be seen in the XPS spectra that the extent and onset temperature of surface reconstruction are different for CH<sub>3</sub>S and DMDS. Further, although the adsorption site of the thiolates and atomic sulfur has been determined,<sup>10,20</sup> the relative positions of these species, as well as surface hydrogen, carbon, and unoccupied metal sites, are not. The structure of this complex ensemble of surface species undoubtedly influences the thiolate decomposition. The isotope effect is not simply a consequence of thiolates adsorbed in 4-fold hollow sites, since Castro et al.<sup>11</sup> saw no isotope effect in the methane desorption when CH<sub>3</sub>SH was adsorbed on hydrogen- and deuterium-covered Ni(100).

The third methane formation process at high coverage in the temperature range 300–450 K involves a disproportionation reaction between the remaining surface methyl thiolates, accompanied by reaction-limited H<sub>2</sub> desorption in the 300–500 K range. During the decomposition of CH<sub>3</sub>SH on Ni(100), reaction-limited H<sub>2</sub> desorption is observed above 400 K in a series of well-defined peaks.<sup>11</sup> Castro et al. attributed this desorption to the decomposition of thiolate and hydrocarbon fragments on the surface. The production of methane at high temperature from DMDS on Ni(111) may be related to the higher coverage that inhibits total decomposition. The high-temperature methane desorption is also related to the lack of surface hydrogen, since it disappears in the presence of preadsorbed H<sub>2</sub> or D<sub>2</sub>. The high-temperature methane desorption is not a direct consequence of the reconstruction and the presence of methyl thiolate in 4-fold sites, since the formation of methane from either methanethiol or DMDS<sup>22</sup> is complete by 300 K on Ni(100). The high-temperature methane desorption from DMDS on Ni(111) most likely results from thiolate disproportionation (limited by C–H bond activation), hydrogenation of hydrocarbon fragments, or both.

The C 1s peak area analysis suggests that by 550 K approximately 15% of the adsorbed C in methyl thiolate decomposes nonselectively to atomic components, while the remaining 85% desorbs mostly as gaseous methane and ethane. For an ideally clean reaction where the maximum amount of methane is produced, the upper limit would be 75% methane production and no hydrogen desorption, since one methyl group would supply three hydrogens to make three methane molecules. However, small amounts of C<sub>2</sub>H<sub>6</sub> are formed that do not need additional hydrogen, plus possible contributions of hydrogen from the ambient can explain the deficiency in surface carbon and the desorption of H<sub>2</sub>. In addition, the amount of carbon detected by XPS following annealing at 550 K is likely to be less than the total amount of atomic carbon from DMDS, since carbon is known to dissolve into the bulk upon annealing. The selectivity to methane formation from methanethiol on clean Ni(111) is approximately 80%.

A direct comparison of the integrated methane desorption intensities (measured under the same conditions) indicates that about 40% more methane is produced from DMDS than from methanethiol on Ni(111). This increase is mainly due to the 32% higher methyl thiolate coverage in the case of DMDS. However, the desorption data suggest a somewhat higher selectivity for DMDS.

As in the case of methanethiol adsorption on Ni(111), postadsorption of hydrogen makes no significant change in the methane desorption process. This is attributed to methyl thiolate blocking the adsorption of hydrogen.<sup>2,29</sup>



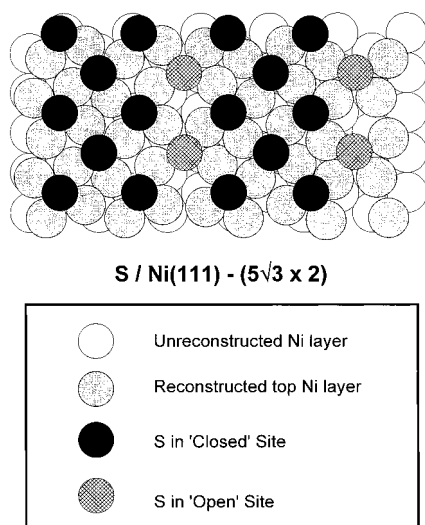


**Figure 10.** Surface model for the ( $5\sqrt{3} \times 2$ ) S structure from 0.40 ML of S on Ni(111).<sup>20,26</sup>

**Surface Reconstruction.** Consideration of surface reconstructions must be included in the interpretation of the DMDS reaction chemistry. The Ni(111) surface is known to reconstruct when exposed to large coverages of atomic S or atomic C.<sup>30,31</sup> The general type of reconstruction is the same for both adsorbates: the 3-fold sites on the hexagonal (111) surface convert into 4-fold sites that locally have a (001)-like configuration. STM<sup>32</sup> and X-ray scattering<sup>26</sup> data indicate that atomic S induces a periodic rotation of the 4-fold cells, which results in an "open" channel every fifth row (Figure 10). Atomic C apparently only produces the 4-fold reconstruction.<sup>31</sup> These reconstructions have been attributed to compressive surface stress induced by the adsorbates.<sup>31</sup> The LEED patterns observed after annealing DMDS adsorbed on Ni(111) surfaces immediately suggest the surface undergoes reconstruction. A saturation coverage of DMDS annealed above 500 K resulted in LEED patterns consistent with a ( $5\sqrt{3} \times 2$ ) S surface structure, like that observed from the highest S coverages obtained from H<sub>2</sub>S/Ni(111).<sup>20</sup> In contrast, DMDS coverages as low as 0.15 ML produced weak, complex LEED patterns possibly resulting from a mixture of ( $5\sqrt{3} \times 2$ ) S and  $c(5\sqrt{3} \times 9)$  rect C<sup>30</sup> structures. The patterns observed were very sensitive to the coverage and annealing conditions.

The S 2p binding energies from atomic S that forms during the decomposition of DMDS are also clearly indicative of surface reconstruction. The correlation between the S 2p binding energy and the type of adsorption site for CH<sub>3</sub>S and S on Ni surfaces has been firmly established by more direct structural probes such as ion scattering<sup>20</sup> and photoelectron diffraction.<sup>10,28</sup> As seen in Figure 5, atomic S is present in both 3-fold and reconstructed 4-fold sites as indicated by features at 161.15 and 161.55 eV, respectively. S in the reconstructed sites is evident at 250 K for both 0.25 and 0.33 ML of DMDS, indicating that the reconstruction commences at low temperature. The coverage of atomic S that is present during the initial stages of decomposition is insufficient to induce reconstruction by itself, since previous studies indicate that up to 0.25 ML of atomic S can be adsorbed on the Ni(111) surface without inducing reconstruction.<sup>20</sup> Apparently, atomic S, atomic C, and CH<sub>3</sub>S can collectively result in reconstruction. By 600 K, with only atomic C and S on the surface, a single S state is present that has a binding energy indicative of adsorption in a "closed" 4-fold site.<sup>20</sup> The atomic C apparently inhibits adsorption of S in the "open" 4-fold site. When the sample is annealed to 1000

K, the atomic C diffuses into the bulk (see Figure 6) and the surface responds to the atomic S alone. With 0.33 ML of DMDS, the S is observed in both the "open" and "closed" 4-fold hollow sites, which have binding energies of 162.10 and 161.55 eV, respectively. With 0.25 ML of DMDS, annealing to 1000 K resulted in partial restoration of the unreconstructed surface, as evidenced by the presence of S in both unreconstructed 3-fold sites and the reconstructed 4-fold sites. The S 2p spectra and LEED patterns following anneals at 1000 K were very sensitive to small variations in coverage and annealing conditions that result in changes in S and C coverage.

Comparison of the  $\nu(\text{Ni-S})$  losses for the high and low coverages of DMDS with that of saturated methanethiol on Ni(111) provides further confirmation of the reconstruction. As indicated in Figure 8, the vibrational spectrum for saturated DMDS on the Ni(111) surface annealed above 550 K shows a Ni-S stretching frequency at 315 cm<sup>-1</sup>, similar to the 325 cm<sup>-1</sup> frequency observed for S in the 4-fold sites on the ( $5\sqrt{3} \times 2$ )-S reconstructed surface produced by 0.40 ML of S.<sup>20</sup> The  $\nu(\text{Ni-S})$  loss following treatment at 550 K of 0.15 ML of DMDS on Ni(111) appears at 375 cm<sup>-1</sup>. Ni-S stretch frequencies of about 350 and 365 cm<sup>-1</sup> have been reported previously for the  $c(2 \times 2)$  S (0.50 ML) and  $p(2 \times 2)$  S (0.25 ML) structures on the Ni(100) surface, respectively, where the sulfur is believed to adsorb at the 4-fold site in both instances.<sup>27</sup> For S coverages of  $\leq 0.25$  ML from CH<sub>3</sub>SH, a  $p(2 \times 2)$  LEED structure was observed and the Ni-S stretch is at 390 cm<sup>-1</sup>, which is characteristic of S adsorbed in a 3-fold site.

## Conclusions

The experimental results on the study of dimethyl disulfide on Ni(111) exhibit a number of similarities and contrasts with methanethiol on the same surface. Some molecular adsorption is reported for high coverages of DMDS on the Ni(111) surface at 100 K. However, HREELS and XPS results show that methyl thiolate is the primary surface intermediate and all of the S-S bonds are broken by 150 K. Some methyl thiolate persists to >350 K for 0.33 ML of DMDS on Ni(111). The bonding and orientation of the methyl thiolates from DMDS are believed to be the same as those of the methyl thiolates from CH<sub>3</sub>SH on Ni(111).

The products formed following multilayer DMDS desorption at 166 K are methane, hydrogen, and small amounts of ethane. For low coverages of DMDS a nonselective decomposition reaction is observed, while for high coverages methane formation is the dominant reaction. Disproportionation and coupling reactions between the adsorbed thiolates are proposed for the main reaction mechanisms for methane and ethane formation, respectively. The hydrogen source for the methane formation is decomposed methyl from the thiolate. The 268 K methane formation process is due to the methyl thiolate adsorbed at 3-fold sites and is rate-limited by C-S bond activation. The methane formation process above 300 K is due to the methyl thiolate at high-coordination sites and is limited by C-H bond formation. DMDS forms 32% higher S coverages and 40% more methane than methanethiol, and up to 85% of the adsorbed DMDS is converted to hydrocarbon. The ( $5\sqrt{3} \times 2$ )-S structure observed for saturation amounts of DMDS starts below 300 K and for thiolate coverages as low as 0.15 ML.

## References and Notes

- Friend, C. M.; Chen, D. A. *Polyhedron* **1997**, *16*, 3165.
- Rufael, T. S.; Huntley, D. R.; Mullins, D. R.; Gland, J. L. *J. Phys. Chem.* **1995**, *99*, 11472.

- (3) Huntley, D. R. *J. Phys. Chem.* **1989**, 93, 6156.  
(4) Mullins, D. R.; Lyman, P. F. *J. Phys. Chem.* **1993**, 97, 9226.  
(5) Mullins, D. R.; Lyman, P. F. *J. Phys. Chem.* **1993**, 97, 12008.  
(6) Mullins, D. R.; Lyman, P. F. *J. Phys. Chem.* **1995**, 99, 5548.  
(7) Wiegand, B. C.; Uvdal, P.; Friend, C. M. *Surf. Sci.* **1992**, 279, 105.  
(8) Parker, B.; Gellman, A. *Surf. Sci.* **1993**, 292, 223.  
(9) Rufael, T. S.; Koestner, R. J.; Kollin, E. B.; Salmeron, M.; Gland, J. L.; *Surf. Sci.* **1993**, 297, 27.  
(10) Mullins, D. R.; Huntley, D. R.; Tang, T.; Saldin, D. K.; Tysoe, W. T. *Surf. Sci.* **1997**, 380, 468.  
(11) Castro, M. E.; Ahkter, S.; Golchet, A.; White, J. M. *Langmuir* **1991**, 7, 126.  
(12) Castro, M. E.; White, J. M. *Surf. Sci.* **1991**, 257, 22.  
(13) Nuzzo, R. G.; Zegarski, B. R.; Dubois, L. H. *J. Am. Chem. Soc.* **1987**, 109, 733.  
(14) Sexton, B. A.; Nyberg, G. L. *Surf. Sci.* **1987**, 165, 251.  
(15) Bao, S.; McConville, C. F.; Woodruff, D. P. *Surf. Sci.* **1987**, 187, 133.  
(16) Seymour, D. L.; Bao, S.; McConville, C. F.; Crapper, M. D.; Woodruff, D. P.; Jones, R. G. *Surf. Sci.* **1987**, 189/190, 529.  
(17) Edmonds, T.; McCarroll, J. H.; Pitkethly R. C. *J. Vac. Sci. Technol.* **1971**, 8, 68.  
(18) Fernández, A.; Espinos, J. P.; González-Elipé, A. R.; Kerkar, M.; Thompson, P.; Lüdekke, J.; Scragg, G.; de Carvalho, A. V.; Woodruff, D. P.; Fernández-García, M.; Conesa, J. C. *J. Phys.: Condens. Matter* **1995**, 40, 7781.  
(19) Ku, Y.; Overbury, S. H. *Surf. Sci.* **1992**, 276, 262.  
(20) Mullins, D. R.; Huntley, D. R.; Overbury, S. H. *Surf. Sci.* **1995**, 323, L287.  
(21) Perdureau, M.; Oudar, J. *Surf. Sci.* **1970**, 20 (80), 168.  
(22) Rufael, T. S.; Gland, J. L. Unpublished work of DMDS on Pt(111) and Ni(100).  
(23) Winkler, A.; Rendulic, K. D. *Surf. Sci.* **1982**, 118, 19.  
(24) Frankiss, J. G. *J. Mol. Struct.* **1969**, 3, 89.  
(25) Lee, M. B.; Yang, Q. Y.; Ceyer, S. T. *J. Chem. Phys.* **1987**, 85, 2724.  
(26) Foss, M.; Feidenhans'l, R.; Nielsen, M.; Findeisen, E.; Johnson, R. L.; Buslaps, T.; Stensgaard, I.; Besenbacher, F. *Phys. Rev. B* **1994**, 50, 8950.  
(27) Anderson, S.; Karlsson, P. A.; Persson, M. *Phys. Rev. Lett.* **1983**, 51, 2378.  
(28) Mullins, D. R.; Tang, T.; Chen, X.; Shneerson, V.; Saldin, D. K.; Tysoe, W. T. *Surf. Sci.* **1997**, 372, 193.  
(29) Vajo, J. J.; McCarty, J. G. *Appl. Surf. Sci.* **1991**, 47, 23.  
(30) Gardin, D. E.; Batteas, J. D.; Van Hove, M. A.; Somorjai, G. A. *Surf. Sci.* **1993**, 296, 25.  
(31) Grossman, A.; Erley, W.; Ibach, H. *Surf. Sci.* **1995**, 337, 183.  
(32) Ruan, L.; Stensgaard, I.; Besenbacher, F.; Laesgaard, E. *Phys. Rev. Lett.* **1993**, 71, 2963.